Molecular Neurobiology (2024) 61:6599–6612
https://doi.org/10.1007/s12035-024-03997-w

ORIGINAL ARTICLE

Restoration of nNOS Expression Rescues Autistic-Like Phenotypes Through Normalization of AMPA Receptor-Mediated Neurotransmission

Xiaona Wang[1] · Yaodong Zhang[1] · Shuying Luo[1] · Ke Zhao[1] · Chao Gao[2] · Daoqi Mei[3] · Yongtao Duan[1] · Shunan Hu[1]

Received: 28 October 2023 / Accepted: 27 January 2024 / Published online: 8 February 2024

Abstract

Autism spectrum disorder (ASD) is associated with a range of abnormalities characterized by deficits in socialization, communication, repetitive behaviors, and restricted interests. We have recently shown that neuronal nitric oxide synthase (nNOS) expression was decreased in the basolateral amygdala (BLA) of mice after postnatal valproic acid exposure. Neuronal activity-regulated pentraxin (Narp) could contribute to the regulation of the GluA4 2-amino-3-(5-methyl-3-oxo-1,2-oxazol-4-yl) propanoic acid (AMPA) subunits which are predominantly expressed in interneurons. However, the specific role of nNOS re-expression on excitatory neurotransmitter with relevance to ASD core symptoms in VPA-treated animals remains to be elucidated. Herein, nNOS overexpression using a lentiviral vector and L-arginine-activating PI3K-Akt-mTOR signaling can restore nNOS expression in the BLA induced by VPA. Restoration of nNOS expression in these mice was sufficient to reduce the severity of ASD-like behavioral patterns such that animals exhibited decreases in abnormal social interactions and communication, stereotyped/repetitive behaviors, and anxiety-like traits. Most strikingly, re-expression of nNOS upregulated surface expression of Narp and GluA4 in nNOS-positive interneuron as shown by immunoprecipitation and Western blotting. Whole-cell patch-clamp recordings demonstrated that restoration of nNOS had a significant enhancing effect on AMPA receptor-mediated excitatory glutamatergic synaptic neurotransmission, which was inhibited by disturbing the interaction between Narp and GluA4 in acutely dissociated BLA slices. Overall, these data offer a scientific basis for the additional study of nNOS re-expression as a promising therapeutic target by correcting AMPA receptor-mediated synaptic function in ASD and related neurodevelopmental disorders.

Keywords Autism spectrum disorder · Neuronal nitric oxide synthase · Interneuron · Excitatory neurotransmission · AMPA receptor subunit GluA4

Introduction

Autism spectrum disorders (ASD) are an early neurodevelopmental syndrome associated with deficits in impaired or abnormal social interactions and restricted range of interests or repetitive behaviors [1]. Several brain structures and functions have been demonstrated to underlie the manifestation of ASD-like symptoms, including the basolateral amygdala (BLA) [2, 3]. An overwhelming body of clinical and experimental evidence suggests that ASD is linked with synaptic alterations of excitatory system in critical areas of the brain controlling social communication and repetitive behaviors [4, 5]. Indeed, converging evidence shows that glutamate-mediated excitatory synaptic transmission by the neurotransmitter a-amino-3-hydroxy-5-methyl-4-isoxazolepropionic acid (AMPA) is severely impaired in some

✉ Xiaona Wang
xiaonawang2015@163.com

[1] Henan Children's Hospital, Zhengzhou Children's Hospital, Henan Key Laboratory of Children's Genetics and Metabolic Diseases, Henan Children's Neurodevelopment Engineering Research Center, Children's Hospital Affiliated to Zhengzhou University, Zhengzhou, China

[2] Department of Rehabilitation, Children's Hospital Affiliated to Zhengzhou University, Zhengzhou, China

[3] Department of Neurology, Children's Hospital Affiliated to Zhengzhou University, Zhengzhou, China

ASD animal models [5, 6]. Pharmacological enhancement of AMPA receptor function is effectively reported to rescue ASD-associated behavioral defects [7].

Several different strains of mouse, expressing ASD-associated behaviors, were used to show abnormalities in trafficking of AMPA receptors [8]. GluA4-containing AMPA receptors are mainly expressed in the inhibitory interneurons of the BLA of animal models [9–11]. Notably, neuronal activity-regulated pentraxin (Narp) is belonging to a member of the neuronal pentraxin family and interacts with the extracellular N-terminal domain of the GluA4 subunit generating AMPA receptor clusters in the postsynaptic membrane of PV-positive interneurons [12]. Knockdown of Narp abolished retrieval enhanced glutamatergic transmission [13]. The upregulation of Narp recruited AMPA receptors from the neuronal membrane to enhance excitatory synaptic transmission [13]. Nevertheless, it is presently undetermined that excitatory neurotransmitter and expression of ionotropic glutamate receptor subunits in interneurons trigged by neuronal nitric oxide synthase (nNOS) re-expression are affected in VPA-treated animals.

We have previously shown that nNOS-expressing interneurons are predominantly expressed in the BLA of rodents [14] and strongly implicated in ASD-related phenotypes [15]. Multiple lines of evidence indicate that nNOS-containing cells are involved in the regulation of synaptic transmission [16, 17]. We reported excitatory synaptic input onto nNOS interneurons in hippocampus [18]. We have also recently demonstrated that nNOS expression was reduced in the BLA of mice after postnatal valproic acid exposure [19]. Further, proteomic data that we obtained for the Narp and GluA4 surface expression demonstrated the prominent decrease in nNOS interneurons in mice treated with VPA [10]. Drawing on these findings, therefore, we hypothesize that surface Narp and GluA4 synergistically are involved in the regulation of excitatory glutamatergic synaptic transmission of nNOS re-expression in VPA-exposed animals, which contributes to mitigation of behavioral dysfunction in ASD.

There is mounting evidence from clinics as well as animal models for the role of PI3K-AKT-mTOR in synaptic function when hypoactivated associated with ASD-like behavioral abnormalities [20, 21]. Herein, we first examined the behavioral alternations in recombinant lentivirus (LV)-mediated overexpression of nNOS and L-arginine (L-Arg, substrate for nNOS) treatment-activating PI3K-Akt-mTOR signaling in VPA-treated mice. Then, the changes in GluA4 interaction with Narp, GluA4 surface expression, and excitatory synaptic transmission in mice induced by restoration of nNOS within the BLA were studied. It is indicated that the nNOS re-expression contributes to alleviation of a spectrum of phenotypes associated with ASD. Interestingly, we observed the dramatic augmentation in AMPA receptor-mediated excitatory neurotransmission, consistent with increased GluA4 surface levels by protein–protein interaction with Narp in nNOS re-expression-treated mice. Overall, our results demonstrated nNOS re-expression may represent a viable approach to treating ASD.

Materials and Methods

Animals

Male C57BL/6 J wild-type mice and nNOS-GFP mice (stock no. 014541, Jackson Laboratory) [10] were housed singly in standard laboratory cages in a temperature (23–25 °C) and humidity (50–60%) controlled vivarium with a 12-h light/12-h dark cycle. Food and water were provided ad libitum throughout the experiment. All experiments were done in accordance with Zhengzhou University and international guidelines on the ethical use of animals. All efforts were made to minimize animal suffering and reduce the amount of animal suffering.

Drug Treatment and Experimental Grouping

As we reported previously [19], C57BL/6 J and nNOS-Cre mice were mated and examined for the presence of a vaginal plug, defined by the presence of embryonic day 1 (E1). On E12.5, pregnant female mice were intraperitoneally injected with 600 mg/kg of VPA (Sigma Aldrich, MO, USA) in 0.9% saline, while control injections consisted of equivalent volume of saline solution. On postnatal day 21, their offspring were weaned and transferred to cages. Only male pups were used in subsequent experiments.

A lentivirus encoding nNOS (pLenti-CMV-nNOS-EGFP; 3.25×10^8 Tu/ml) was purchased from Shanghai Biotechnology Co., Ltd., with a virus encoding EGFP (LV-GFP; 3.43×10^8 Tu/ml) serving as a control. Lentiviral injection into the BLA was carried out using our previously published protocol [1]. In brief, animals were intraperitoneally administered pentobarbital sodium (100 mg/kg) and transferred to a stereotaxic apparatus. A glass pipette was then used to infuse 2 µl LV-nNOS and LV-GFP at 0.3 ml/min bilaterally in the BLA (anterior–posterior 1.6 mm, medial–lateral ± 3.5 mm, and dorsal–ventral 4.0 mm). The needle was then allowed to rest in the injection site for 10 min following the completion of the injection to ensure that all viral particles remained within the BLA.

Seven days after the injection of LV vectors, mice were randomly selected from each experimental group and used for immunofluorescence analyses. Western blotting was used to evaluate the efficiency of LV vector interventions, which were also quantified at 21 days.

Immunofluorescence

Immunohistochemical protocols were used in this study, as we have been previously described [1]. Mice were deeply anesthetized and perfusion-fixed transcardially with 4% paraformaldehyde. Brains were removed from the skull and post-fixed overnight at 4 °C and cryoprotected in 30% sucrose. Coronal sections (40 μm) were cut on a vibratome (Leica Microsystems, Mannheim, Germany) in 0.1 M phosphate-buffered saline (PBS). Sections were incubated in a blocking solution that consisted of 3% bovine serum albumin, 0.3% Triton X-100, and 2% goat serum in 0.1 M PBS. After that, sections were incubated with anti-GFP (Invitrogen, Carlsbad, CA, USA; Cat#A-11122) in a dilution of 1:1000 at 4 °C overnight. The Alexa Fluor 488-conjugated donkey anti-rabbit immunoglobulin G (Invitrogen; Cat#A-10042) in 1:1000 dilutions was used as secondary antibodies. Sections were washed with PBS and mounted onto gelatin-coated slides. Sections were scanned using the Zeiss 900 laser scanning microscope (Carl Zeiss, Jena, Germany).

Western Blotting

Laser microdissection of BLA of mice was performed using a Laser PALM-Zeiss Microbeam system (PALM, Oberkochen, Germany) configured on an inverted Axio Observer Microscope. The BLA tissues were homogenized in ristocetin-induced platelet aggregation (RIPA) buffer containing protease and phosphatase inhibitors (Beytime, Shanghai, China). Homogenates were sonicated, incubated on ice for 20 min and then centrifuged at 12000 × g for 15 min at 4 °C to precipitate insoluble debris. The supernatants were collected, and protein concentrations were determined using the BCA protein assay kit (Beyotime, Nantong, China). Sample protein concentrations were adjusted to 4 μg/μl for Western blotting. Fifty microgram total protein was separated on 5–12% sodium dodecyl sulfate (SDS)–polyacrylamide gels and transferred to polyvinylidene fluoride (PVDF) membranes (Millipore, Billerica, MA, USA). Membranes were then blocked with 5% nonfat milk in Tris-buffered saline solution containing 0.1% Tween 20 (TBS-T) for 1 h. After blocking, the blots were probed overnight at 4 °C with the following primary antibodies: anti-PI3 kinase p85 alpha (phospho Tyr607) (1:1000, Abcam, Cambridge, MA, USA; Cat#ab182651), anti-PI3 kinase p85 alpha (1:1000, Abcam; Cat#227204), anti-AKT (phospho Thr308) (1:1000, Abcam; Cat#ab38449), rabbit anti-AKT (1:1000, Abcam; Cat#ab308107), anti-mTOR (phospho Ser2448) (1:1000, Abcam; Cat#ab109268), anti-mTOR (1:1000, Abcam; Cat#ab134903), anti-P70 S6 kinase (phospho Thr389) (1:1000, Cell Signaling Technology, Danvers, CT, USA; Cat#9205), anti-P70 S6 kinase (1:1000, Cell signaling technology; Cat#9202), anti-eIF4E (phospho Ser209) (1:1000, Cell Signaling Technology; Cat#9741), anti-eIF4E (1:1000, Cell Signaling Technology; Cat#2067), and anti-nNOS (1:1000, Sigma; Cat#N7280). Membranes were simultaneously probed with mouse monoclonal anti-glyceraldehyde 3-phosphate dehydrogenase antibody (1:1000, GAPDH, Cell Signaling Technology; Cat#5174) as a loading control. After washing with TBS-T, the membrane was incubated with the peroxidase-conjugated anti-rabbit IgG secondary antibody (1:5000, ZSGB-Bio, Beijing, China; Cat#ZB-2301) or anti-mouse IgG secondary antibody (1:5000, ZSGB-Bio; Cat#ZB-2305) at room temperature for 2 h, followed with washing and detection using the enhanced chemiluminescence (ECL) detection kit (Thermo Fisher Scientific, Rockford, IL, USA). Bands were detected using densitometry (Bio-Rad, Hercules, CA, USA) and quantified using densitometric analysis (ImageJ software, NIH).

Behavioral Assessments

At 3 weeks following lentiviral injection and pretreatment with L-arginine (350 mg/kg, i.p.) and NVP-BEZ235 (25 mg/kg, intragastricaly), mice underwent social interaction, self-grooming, marble-burying, and open-field tests on 4 consecutive days. At 24 h after completion of the open-field task, mice were sacrificed for Western blot analysis and received electrophysiological recordings. All behavioral recordings were implemented by camera-assisted ANY-Maze software (Stoelting Co., Wood Dale, IL, USA).

Sociability and Social Novelty Testing

Sociability testing was carried out using a three-chamber black plastic box apparatus as previously published protocol [22]. The three-chamber box (45 × 30 × 20 cm) included dividing walls with 10 × 12 cm openings allowing free access to each chamber. Test mice were correspondingly sex- and strain-matched with novel animals with which they had not received any prior contact. At the start of the test, a selected animal was individually placed in an empty central cage, with the selected novel animal being placed in a wire cage (12 cm diameter) in the left compartment, and an empty wire cage (novel object) being placed in the right chamber. After a 5-min acclimation period, sociability tests were performed for 10 min. For social novelty preference tests, a different unfamiliar mouse was positioned within the wire cage in the right compartment, and the study subject was returned to the empty central cage. Animal movements during the following 10 min were then monitored, which was allowed to freely explore three chambers.

Self-Grooming

Self-grooming testing was conducted for repetitive and compulsive behavior, which is another prominent symptom of ASD [23]. The conditioning chamber is composed of a rectangular box (44 × 22 × 10 cm) with 2 cm of bedding. The time mice spent grooming was counted for 10 min. Grooming behavior included all sequences of face-wiping, scratching/rubbing of head and ears, and full-body grooming.

Marble-Burying Assay

A marble-burying test was used to assess for stereotyped behaviors in mouse model of ASD [24]. A 6-cm layer of chipped cedar wood bedding was applied to the bottom of clean cages (length × wide × height, 30 × 18 × 16 cm). Animals were then added to cages for 10 min. On this, 16 glass marbles (13 mm diameter) were spaced evenly in a 3 × 4 array. The number of marbles that were buried (to at least 2/3 their depth) after 10 min was counted, with digging being considered as coordinated limb movement that displaced the bedding.

Open-Field Test

Open-field tests were performed as in our prior reports [1]. Animals were placed into the central area of a 50 cm (W) × 54 cm (L) × 42 cm (H) chamber, and both the time spent in the central area (16 × 16 cm) and the total distance traveled were calculated for 10 min.

Immunoprecipitation

Immunoprecipitation was used to detect the interaction between Narp and GluA4. Briefly, the BLA tissues were obtained as described above. The supernatant from BLA was collected and supplemented with 40 µl protein A/G-agarose beads (Sigma, USA) overnight at 4 °C on a wheel. The beads were then allowed to sediment at the bottom of the tube, and the supernatant was collected. The anti-Narp (1:1000, Abcam; Cat#305257) and anti-GluA4 (1:1000, Cell signaling technology; Cat#8070) antibodies were incubated in equal amounts with the supernatant. Protein A-/G-agarose beads were added to the supernatant, and the supernatant was incubated for 2 h at room temperature. The beads were then washed 4 times with RIPA buffer (Beyotime) and submitted to SDS-PAGE. The mixture was boiled at 95 °C for 5 min. The Western blots were detected using Narp and GluA4 antibodies for immunoprecipitation.

TAT Peptides

Cell-permeable peptides were synthesized by Shanghai Science Peptide Biological Technology (Shanghai, China) (TAT control, YGRKKRRQRRR-TETWGQRSIE; TAT-GluA4, YGRKKRRQRRR-LGKVAPWSDQ). The peptide was purified by HPLC, and the purity was 98%. In some experiments, peptides (dissolved in saline) were injected into mice tail veins (20 mg/mL) using 25-gauge needle at 30 min before behavioral testing. A scrambled TAT peptide was injected in parallel as controls.

Surface Biotinylation

Surface proteins of nNOS-expressing interneurons in the BLA were performed as we described earlier [10], which were prepared with a Mem-PER Plus Membrane Protein Extraction Kit (Thermo scientific, Waltham, MA). Briefly, the BLA tissues were rinsed with ice-cold PBS containing 1 mM $MgCl_2$ and 0.01 mM $CaCl_2$ and then incubated on ice with PBS/$MgCl_2$/$CaCl_2$ containing 1 mg/ml Sulfo-NHS Biotin (Pierce, Rockford, Illinois, USA) for 45 min. The tissues were rinsed with 100 mM glycine to quench unreacted biotin. nNOS-containing interneurons were scraped in ice-cold lysis buffer (in mM, 150 NaCl, 50 Tris–HCl pH 7.5, 1% Triton X-100, 10 sodium pyrophosphate, 10 EDTA, 0.2% SDS, 50 NaF, and protease inhibitors) and then sonicated and centrifuged for 20 min. To detect the total expression of GluA4, 10% of the cell lysate was boiled at 98 °C for 10 min in SDS-containing buffer with 5% β-mercaptoethanol. To detect the surface expression of GluA4, 80% of the cell lysate was added to streptavidin magnetic beads (Pierce, Rockford, Illinois, USA) and rotated at 4 °C for 2 h. After 4 times of washing, the precipitated sample was resolved via SDS-PAGE and immunoblotting using the indicated antibodies.

Slice Electrophysiology

Whole-cell patch-clamp recording was performed as described previously [1, 25, 26]. Mice were anesthetized with isoflurane and transcardially perfused with ice-cold carbogenated (95% O_2, 5% CO_2) cutting solution containing the following (in mM): 75 sucrose, 88 NaCl, 2.5 KCl, 1.26 NaH_2PO_4, 25 $NaHCO_3$, 8 $MgCl_2$, and 0.5 $CaCl_2$ (pH 7.3–7.4, 300–310 mOsm/L). Coronal slices of 300 µm containing the BLA were prepared using a Campden 5100 mz vibrating microtome (Campden Instruments, Loughborough, England). The perfusion flow rate was 2 ml/min. Whole-cell patch-clamp recordings were made under infrared differential interference contrast visualization at 32 °C in artificial cerebral spinal fluid (ACSF) containing the following (in mM): 125 NaCl, 11 glucose, 5 KCl, 25 $NaHCO_3$,

1.25 NaH_2PO_4, 2 $MgSO_4$, and 2.5 $CaCl_2$ (pH 7.3–7.4, 300–310 mOsm/L).

GFP-positive nNOS interneurons in the BLA were held at − 70 mV under a voltage clamp mode to record AMPA miniature excitatory postsynaptic currents (mEPSCs). AMPA-mediated mEPSCs were measured in the presence of tetrodotoxin (TTX, 1 µM), bicuculline (10 mM, Sigma), and D-2-amino-5-phosphonovaleric acid (AP-5, 50 µM, Sigma) from 5 min after establishing the whole-cell configuration. Furthermore, AMPA receptor-evoked EPSCs were recorded from the identified nNOS interneurons in the presence of picrotoxin (100 µM) and AP-5 (50 µM). Membrane voltage was held at + 40 mV. A concentric stimulating electrode (FHC, USA) was placed near the external capsule, 200–250 µm lateral to the recorded cell. Stimulation pulses were given at 0.05 Hz to evoked AMPA receptor-mediated EPSCs. The internal solution in the patch pipette contained the following (in mM): 8 NaCl, 10 HEPES, 0.4 Na_3GTP, 4 Na_2ATP, 10 EGTA, 2 QX-314, 5 4-aminopyridine, 4 $MgCl_2$, 1 $CaCl_2$, and 125 $CsMeSO_4$. After a short washing step in ACSF, the slices were treated with the respective 10 µM TAT fusion proteins. The resistance of patch electrodes was 3–6 MΩ. Data were sampled at 10 kHz and filtered at 2 kHz using an EPC 10 amplifier and Patch

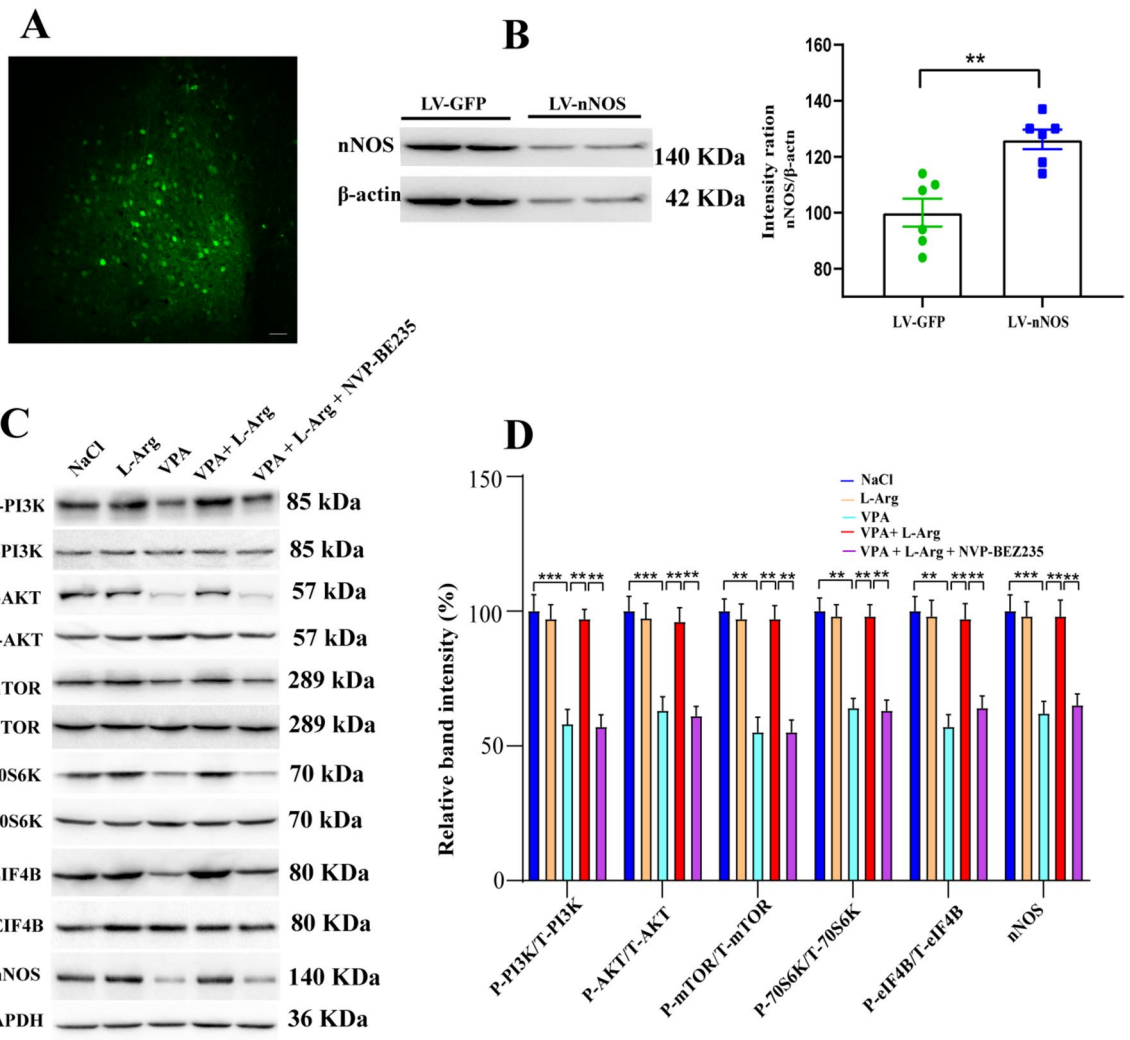

Fig. 1 Confirmation of nNOS re-expression in a mouse model of autism spectrum disorder (ASD). **A** GFP expression indicated by dotted lines in the BLA of VPA-exposed mice was detected on day 7 post-LV injection. **B** nNOS protein levels were measured in nNOS overexpressing of VPA-treated mice on day 21 post-LV injections. Normalized intensity bands for nNOS are presented. Lane 1, LV-GFP-exposed group; lane 2, LV-nNOS-treated group. $n = 6$ mice in each group. $^{**}p < 0.01$. Student's *t*-test. Data are presented as means ± SEM. **C** Representative protein bands of P-PI3K, T-PI3K, P-AKT, T-AKT, P-mTOR, T-mTOR, P-70S6K, T-70S6K, P-eIF4B, T-eIF4B, and nNOS in the BLA. **D** The ratios of phosphorylated P-PI3K/T-PI3K, P-AKT/T-AKT, P-mTOR/T-mTOR, P-70S6K/T-70S6K, P-eIF4B/T-eIF4B, and nNOS expression were determined by western blot in NaCl, L-Arg, VPA, VPA + L-Arg, and VPA + L-Arg + NVP-BEZ235 group. GAPDH was used to evaluate protein loading. $n = 6$ mice for each group. One-way ANOVA followed by Tukey's post hoc test. $^{**}p < 0.01$, $^{***}p < 0.001$. Results are shown as mean ± SEM

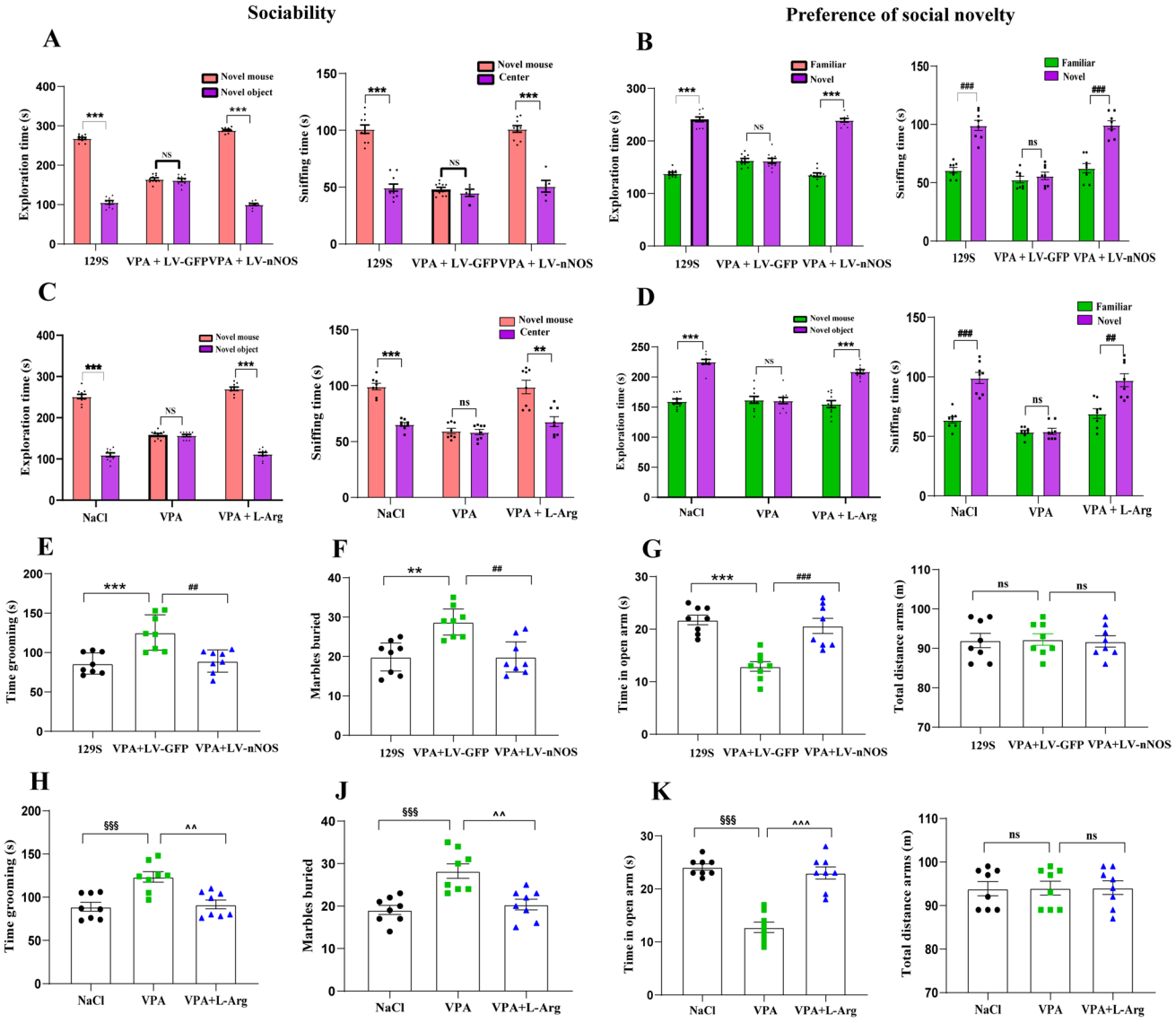

Master 2.54 software (HEKA, Lambrecht, Germany). Series resistance of nNOS interneurons was in the range of 10–20 MΩ and monitored throughout the experiments. If the series resistance changed > 20% during recording, the data were excluded. Data analyses were performed using Mini Analysis Software (Synaptosoft, Decatur, GA, USA).

Statistical Analysis

SPSS 18.0 software was used for all statistical analyses. Data are expressed as mean ± SEM. Data were measured by unpaired two tailed Student's *t*-test for comparison of two groups or one-way ANOVA followed by post hoc Tukey's multiple comparison test. Statistical significance was accepted when $p < 0.05$.

Results

Establishment of Re-expressing nNOS in the BLA

To test the functional importance of nNOS in ASD, we firstly began by overexpressing this protein in VPA-treated mice via the injection of a nNOS-encoding lentivirus into the BLA. On day 7 post-LV injection, GFP signal was evident in the BLA, consistent with successful sustained lentiviral delivery (Fig. 1A). Western blotting further confirmed that nNOS protein levels were significantly increased in VPA-exposed mice that had been injected with LV-nNOS relative to LV-GFP injected control mice at day 21 post-LV injections ($p < 0.01$, Fig. 1B). These results suggested that

◂**Fig. 2** Restoration of nNOS expression enhances mouse social interactions and alleviates stereotyped/repetitive and anxiety-like behaviors. **A**, **C** In an assay testing for social novelty preferences, 129S- and saline-treated mice spent significantly more time in the chamber of the novel mouse relative to the unfamiliar object. In contrast, administration of LV-GFP to VPA and VPA treatment was associated with these animals having spent equal amounts of time in the compartment containing the unfamiliar mouse and the novel object. VPA-treated mice overexpressing nNOS and mice injected with L-Arg spent significantly more time in the chamber of the novel mouse compared to LV-GFP- and VPA-treated animals. In sociability tests analyzing interaction time, 129S- and saline-treated mice spent significantly more time sniffing the novel mouse relative to the unfamiliar object. VPA-exposed mice that had been injected with LV-GFP and L-Arg spent similar amounts of time interacting with the novel mouse and the unfamiliar object. Mice pretreated with LV-nNOS and L-Arg exhibited more interactions with the novel mouse as compared to the novel object. **B**, **D** In an assay testing for social novelty preferences, 129S- and saline-treated mice spent significantly more time in the chamber of the novel mouse compared with the familiar mouse. VPA-exposed mice injected with LV-nNOS and L-Arg preferred exploring the chamber containing the novel mouse compared to familiar controls. In contrast, no significant difference in the time spent exploring the chamber containing the novel mouse was observed relative to the time spent exploring the familiar chamber for VPA-exposed mice treated with LV-GFP and VPA group. Similarly, 129S- and saline-exposed mice spent significantly more time sniffing and engaging with the novel animal compared with the familiar mouse. LV-GFP- and VPA-treated mice spent equal amounts of time sniffing the novel mouse and the familiar animal. VPA + LV-nNOS- and VPA + L-Arg-treated mice exhibited significant increases in the time spent sniffing the unfamiliar mouse as compared to the controls. $^{**}p < 0.01$,$^{***}p < 0.001$ for novel mouse vs. novel object; $^{\#\#}p < 0.01$, $^{\#\#\#}p < 0.001$ for novel side vs. familiar side. ns indicating no statistical significance. $n = 8$ animals per group. One-way ANOVA with Tukey's post hoc test. Data are means ± SEM. **E**, **H** In the self-grooming test, exposure to VPA + LV-GFP and VPA decreased the time spent grooming compared with the 129S and saline-exposed mice, respectively. In VPA-treated mice restoration of nNOS injected with LV-nNOS and L-arginine markedly increased the time spent grooming when compared to corresponding controls. **F**, **J** In a marble-burying test, VPA + LV-GFP and VPA treatment significantly increased numbers of marbles buried when compared to 129S- and saline-exposed group, respectively. VPA-exposed mice exposure to LV-nNOS and L-Arg was associated with a lower number of buried marbles relative to LV-GFP and VPA group. **G**, **K** In the open-field test, treatment with VPA + LV-GFP and VPA was similarly associated with decreased time spent in the open arms relative to 129S- and saline-exposed mice. nNOS re-expressing by treatment with LV-nNOS and L-Arg in the VPA-exposed mice was similarly associated with increased time spent in the open arms relative to LV-GFP- and VPA-treated animals, whereas total distance traveled among groups was unchanged. $n = 8$ mice for each group. $^{**}p < 0.01$, $^{***}p < 0.001$ vs. the 129S group; $^{\#\#}p < 0.01$, $^{\#\#\#}p < 0.001$ vs. the VPA + LV-GFP group; $^{\S\S\S}p < 0.001$ vs. the saline-exposed group; $\wedge\wedge p < 0.01$, $\wedge\wedge\wedge p < 0.001$ vs. the VPA group; ns indicates no statistical significance; one-way ANOVA. Data are shown as means ± SEM

our lentiviral vector was able to successfully enhance nNOS protein expression in cells within the BLA in vivo.

The mice were also divided into five group, including saline group, L-arginine group, VPA group, VPA plus L-arginine, and VPA plus L-arginine plus NVP-BEZ235 as well. He et al. demonstrated a significant increase enhancement of nNOS protein expression after intraperitoneal administration of L-arginine [27]. Further, we investigated whether L-arginine treatment could alter nNOS expression through PI3K-AKT-mTOR pathway in VPA-treated mice. As expected, we show substantially increased nNOS expression in the BLA of VPA-exposed mice after injection of L-arginine. NVP-BEZ235, a novel dual inhibitor of PI3K and mTOR, inhibited augmented nNOS levels through PI3K-AKT-mTOR-p70S6K/eIF4B signal pathway ($p < 0.01$, $p < 0.001$, Fig. 1C–D). Consequently, our observations support the idea that L-arginine upregulates nNOS expression through PI3K-AKT-mTOR signal pathway in these experimental mice.

Alleviation of Impaired Sociability and Social Novelty Response Induced by Restoring nNOS Expression

To examine the influences of nNOS re-expression on behavioral alterations in mouse model of ASD, we next evaluated their performance in tests assigned to measure social behaviors, as impairments in social interaction are a cardinal feature of ASD in humans [28]. As shown in Fig. 2A and C, the results of a post hoc analysis performed using Tukey's test indicated that 129S- and saline-treated mice spent significantly more time in the chamber of the unfamiliar animal compared to the novel object ($p < 0.001$, $p < 0.001$). In sociability tests following VPA exposure, we determined that LV-nNOS and L-arginine-treated mice spent more time in the compartment containing a novel mouse relative to the empty chamber ($p < 0.001$, $p < 0.001$). In contrast, this was not true for mice treated with VPA + LV-GFP and VPA, respectively ($p > 0.05$, $p > 0.05$).

The total time spent sniffing the novel animal and unfamiliar object in each experimental condition was additionally assessed for these experimental mice. As illustrated in Fig. 2A and C, 129S- and saline-exposed mice spent remarkably more time sniffing the novel animal compared to the unfamiliar object ($p < 0.01$, $p < 0.001$). In the VPA-induced ASD mouse model, LV-nNOS- and L-arginine-treated mice also spent more time closely interacting with the novel animal ($p < 0.001$, $p < 0.01$). LV-GFP- and VPA-exposed mice did not display any particular preference, in accordance with a lack of interest in the unfamiliar mouse ($p > 0.05$, $p > 0.05$). Hence, these results suggest that nNOS re-expression can reverse altered interactions in the VPA-induced rodent model of ASD.

Furthermore, the time spent in individual chambers during social novelty preference testing was also assessed. Noticeably, 129S- and saline-exposed mice spent more time in the compartment of the novel mouse relative to that of the familiar animal ($p < 0.001$, $p < 0.001$, Fig. 2B and D). No corresponding differences were detected in the amount of time spent exploring these two compartments among

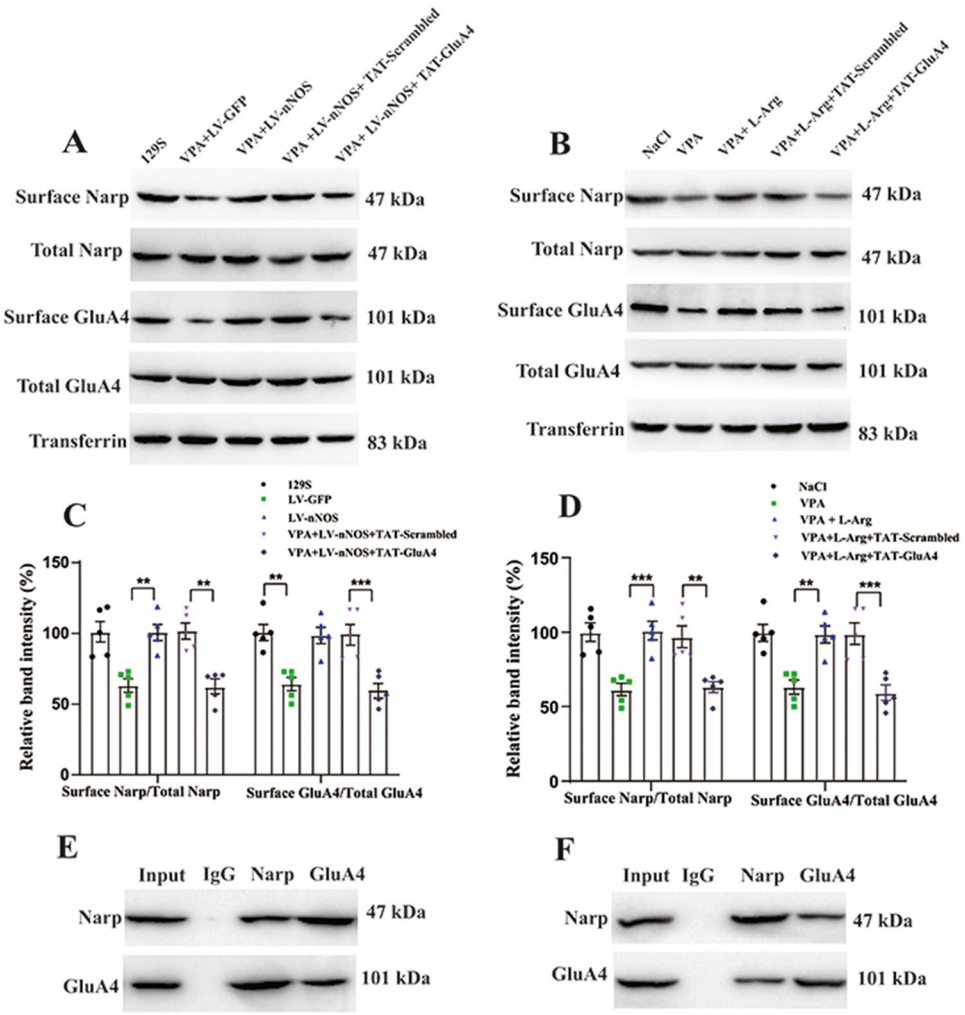

Fig. 3 nNOS re-expression upregulates surface expression of Narp and GluA4 in VPA-treated mice. **A**–**D** Western blot analysis of the surface expression of Narp and GluA4 in the BLA tissues from in VPA-treated mice exposure to LV-nNOS (**A**) and L-arginine treatment (**C**). **B** For the purposes of quantification, relative band intensity of surface Narp/total Narp and surface GluA4/total GluA4 in VPA-treated mice of for 129S, VPA + LV-GFP, VPA + LV-nNOS, VPA + LV-nNOS + TAT-scrambled, and VPA + LV-nNOS + TAT-GluA4 group. **D** Relative band intensity of surface Narp/total Narp and surface GluA4/Total GluA4 in VPA-treated mice of for NaCl, VPA, VPA + L-Arg, VPA + L-Arg + TAT-scrambled, and VPA + L-Arg + TAT-GluA4 group. $n = 6$, one-way ANOVA followed by Tukey's post hoc test. $^{**}p < 0.001$, $^{***}p < 0.001$. Results represent mean ± SEM. **E**–**F** Immunoprecipitation of VPA-treated mice in BLA tissue lysates. Narp co-immunoprecipitates with GluA4 in VPA-exposed mice exposure to LV-nNOS (**E**) and L-arginine treatment (**F**). $n = 6$

VPA + LV-GFP- and VPA-treated mice ($p > 0.05$, $p > 0.05$, Fig. 2B and D). However, VPA-treated mice injected with LV-nNOS and L-arginine preferred exploring the chamber containing the novel animal ($p < 0.001$, $p < 0.001$, Fig. 2B and D).

As shown in Fig. 2B and D, active interactions (based on sniffing time) in the individual chambers in animals were additionally calculated. 129S- and saline-treated mice spent significantly more time sniffing and engaging with a novel mouse compared to a familiar animal ($p < 0.001$, $p < 0.001$). LV-nNOS and L-arginine injection was associated with mice having spent more time interacting with the unfamiliar animal relative to the familiar mouse ($p < 0.001$, $p < 0.01$). In contrast, VPA + LV-GFP- and VPA-treated mice spent a similar amount of time sniffing the novel animal and the familiar mouse ($p > 0.05$, $p > 0.05$). Overall, these data were in line with the findings of the sociability test, suggesting that nNOS re-expression can remediate altered social novelty preferences in these experimental mice.

nNOS Re-expression Attenuates Stereotyped/Repetitive and Anxiety-Like Behaviors

The self-grooming and marble-burying tests were adopted to study repetitive and compulsive-like behaviors [24, 29]. In the self-grooming test, VPA + LV-GFP and VPA treatment substantially increased the time spent grooming compared with the corresponding controls, respectively ($p < 0.001$, $p < 0.001$, Fig. 2E and H). In VPA-treated mice, restoration of nNOS expression injected by LV-nNOS and L-arginine markedly decreased the time spent grooming when compared to LV-GFP and VPA group ($p < 0.01$, $p < 0.01$, Fig. 2E and H). Furthermore, in the marble-burying test, exposure to VPA + LV-GFP and VPA significantly increased the numbers of marbles buried compared with 129S- and saline-exposed group, respectively ($p < 0.01$, $p < 0.001$, Fig. 2F and J). nNOS re-expression by treatment with LV-nNOS and L-arginine in the VPA exposure model was also associated with reduced numbers of marbles buried relative to lentiviral and VPA treatment ($p < 0.01$, $p < 0.01$, Fig. 2F and J).

As shown in Fig. 2G and K, we next conducted open-field tests in which the re-expression of nNOS by treatment with LV-nNOS and L-arginine in VPA-treated mice was associated with increased time spent in the center of the open-field compared with injection with lentiviral and VPA ($p < 0.001$, $p < 0.001$). Treatment with VPA + LV-GFP and VPA remarkably decreased the time spent in the center of the open-field relative to controls ($p < 0.001$, $p < 0.001$). The total distance traveled in these groups was also comparable ($p > 0.05$, $p > 0.05$). Together, our data from animal models of ASD confirm that nNOS re-expression can relieve core ASD-related phenotypes including repetitive and anxiety-like behaviors.

nNOS Re-expression Upregulate Surface Expression of GluA4

Further, we have recently demonstrated that AMPA receptors GluA4 subunits are decreased in association with ASD-like phenotypes [10]. Accumulating evidence suggests that GluA4 receptor subunits are transported by membrane trafficking [12, 30]. To determine whether nNOS re-expression altered GluA4 trafficking, we compared Narp and GluA4 expression in surface and total by Western blot. As shown in Fig. 3A–D, in VPA-treated mice, a significant increase in surface expression of Narp and GluA4 was observed in the LV-nNOS and L-arginine treatment group compared with the LV-GFP and VPA group ($p < 0.01$, $p < 0.001$, $p < 0.01$, $p < 0.01$). In contrast, TAT-GluA4 peptides blocked enhancement in surface Narp and GluA4 expression after injection of LV-nNOS and L-arginine as compared with TAT-scrambled-exposed mice, respectively ($p < 0.01$, $p < 0.001$, $p < 0.01$, $p < 0.001$). The total Narp and GluA4 subunit expression was unchanged ($p > 0.05$, $p > 0.05$). These data suggest that nNOS re-expression does not affect overall Narp and GluA4 expression but instead alters Narp and GluA4 subcellular localization.

A direct interaction could strongly alter GluA4 surface trafficking [12]. Thus, we tested the binding between Narp and GluA4 in vivo by coimmunoprecipitation experiments in VPA-treated mice exposure to LV-nNOS and L-arginine treatment. The results indicated coimmunoprecipitation of Narp and GluA4 by anti-Narp antibodies, demonstrating the interaction of Narp and GluA4, and this interaction was validated by reciprocal coimmunoprecipitation of these two proteins by anti-GluA4 antibodies (Fig. 3E and F). Taken together, these results clearly demonstrate that a stable association between both Narp and GluA4 is required for their postsynaptic trafficking.

Re-expression of nNOS Corrects AMPA-Mediated Miniature EPSCs

It has been demonstrated that AMPA receptor hypofunction in mice was associated with deficits in social and communicative functioning as well as elevated repetitive behaviors [6, 7] and alterations in GluA4 receptor subunits probably contribute to excitatory neurotransmission. We assessed whether the nNOS re-expression can affect AMPA-mediated miniature excitatory postsynaptic currents (AMPA mEPSCs) of nNOS-positive interneurons in the BLA. As illustrated in Fig. 4A–D, using whole-cell patch recording of acute brain slices, we observed a significant augmentation of AMPA mEPSC frequencies and amplitudes in nNOS-containing interneurons of VPA-treated animals injected with LV-nNOS and L-arginine as compared with LV-GFP and VPA group ($p < 0.001$, $p < 0.001$). Conversely, TAT-GluA4 peptides blocked enhancement in frequency and amplitude of AMPA mEPSCs as compared to TAT-scrambled-exposed mice, respectively ($p < 0.001$, $p < 0.001$). Thus, our observations support the idea that restoration of nNOS expression rescues AMPA-mediated mEPSCs via increased surface expression of GluA4 receptors.

Enhancement in Evoked AMPA-Mediated Excitatory EPSCs Induced by nNOS Re-expression

We further assessed whether the restoration of nNOS expression can impact AMPA-mediated evoked excitatory postsynaptic currents (eEPSCs) in VPA-treated animals. nNOS re-expression resulted in significant increases in AMPA receptor-mediated eEPSC amplitudes in nNOS interneurons of VPA-exposed mice in LV-nNOS and L-arginine treatment group compared with the LV-GFP and VPA group ($p < 0.001$, $p < 0.001$, Fig. 5A and B). In contrast, TAT-GluA4 peptides blocked enhancement of evoked AMPA receptor-mediated EPSC amplitude with administration of LV-nNOS and L-arginine compared to TAT-Scrambled-exposed mice ($p < 0.001$, $p < 0.001$, Fig. 5C and D). These experiments demonstrated that nNOS re-expression upregulates evoked GluA4-containing AMPA-mediated synaptic responses by increased surface expression of GluA4 receptors in mouse models of ASD.

Discussion

Here, we show that overexpression of nNOS and L-arginine supplementation activating PI3K-AKT-mTOR signaling prevents behavioral aberrations in mouse model of ASD. Of particular note, restoration of nNOS enhanced surface expression of Narp and GluA4 in nNOS-positive interneuron in theses experimental animals. At the synaptic level, restoring nNOS also reverted AMPA receptor-mediated excitatory transmission, which was suppressed by interrupting the interaction between Narp and GluA4. Together, our data further the understanding of the molecular mechanisms underlying the effect of nNOS re-expression and verify the efficacy and breadth of its application as a potential treatment strategy for ASD.

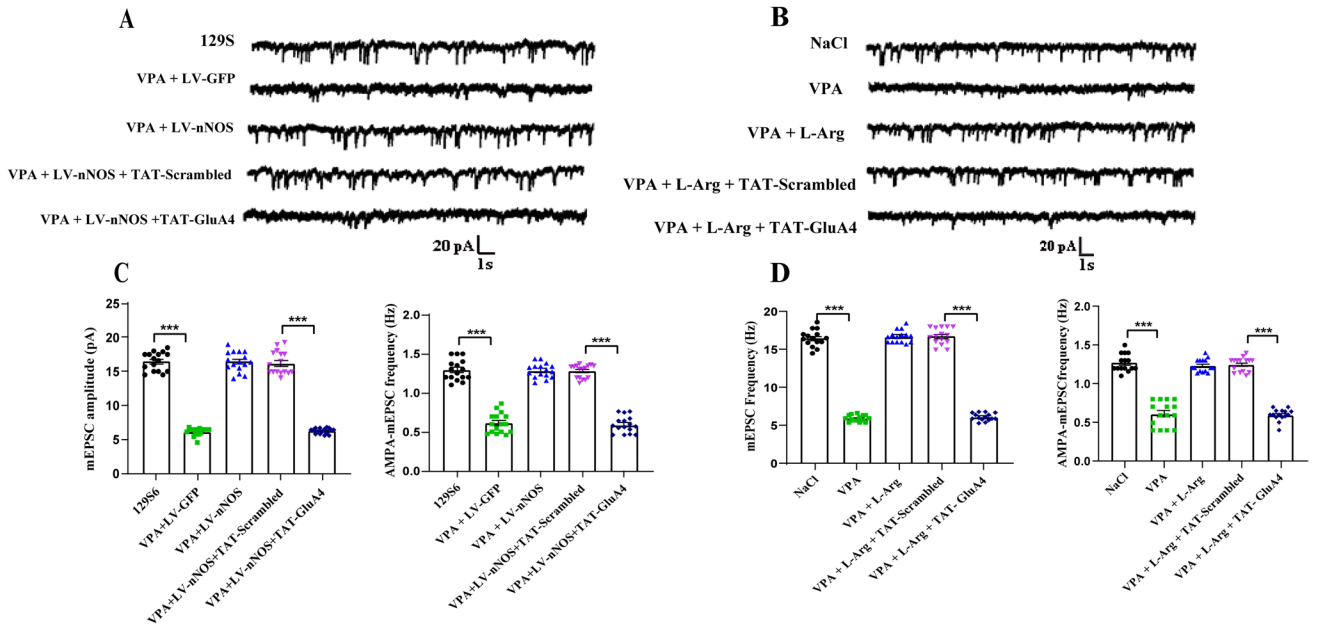

Fig. 4 nNOS re-expression enhances AMPA-mediated miniature excitatory postsynaptic currents(AMPA mEPSCs) in nNOS-positive interneurons of VPA-treated mice. Continuous recordings of AMPA mEPSCs (**A**) and summary graphs showing the amplitude and frequency (**B**) for 129S, VPA + LV-GFP, VPA + LV-nNOS, VPA + LV-nNOS + TAT-scrambled, and VPA + LV-nNOS + TAT-GluA4 group. Representative traces of AMPA mEPSC (**C**) and summary graphs showing the amplitude and frequency (**D**) of AMPA mEPSCs for NaCl, VPA, VPA + L-Arg, VPA + L-Arg + TAT-scrambled, and VPA + L-Arg + TAT-GluA4 group. $n = 17$ slices from 6 mice in each group. $^{***}p < 0.001$ one-way ANOVA. Data are shown as means ± SEM

Our recent results showed the decreased nNOS expression in the BLA of VPA-treated animals. In the current study, our lentiviral vector could successfully enhance nNOS protein expression in cells within the BLA in vivo. Further, mounting evidence indicates that hypoactive PI3K-AKT-mTOR signaling pathway which impacts synaptic function contributes to ASD-like behavioral deficits [20, 21, 31, 32]. The decreased phosphorylated and total PI3K, AKT, mTOR, p70S6K, and total eIF4B protein expression in idiopathic autistic individuals and valproic acid-exposed animals were found [33, 34]. Hyperactive AKT-mTOR pathway was as a therapeutic target for in Cntnap2-deficient mice model of ASD [35]. Moreover, intraperitoneally administered L-arginine, the nNOS protein content was drastically elevated as measured by Western blot analysis [27]. In line with previous results, we found L-arginine supplement can upregulate nNOS expression by activation of PI3K-AKT-mTOR pathway.

We next tested how restoration of nNOS expression in the BLA may affect behavioral disturbances. Hallmark symptoms of ASD encompass impairment in social behaviors [36]. A large amount of data has demonstrated that impaired sociability and preference for social novelty in the animal model of ASD induced by exposure to VPA [1, 37]. Previous studies have established that low levels of PI3K-AKT-mTOR are correlated with the severity of ASD symptoms [31, 32, 38] and the effect on social behaviors in mouse models [39, 40]. Consistent with this notion, our experiments indicated that re-expression of LV-nNOS and L-arginine treatment-activating PI3K-AKT-mTOR signaling pathway also showed improvements in social engagement and preference for a social stimulus in mouse model of ASD. Together, these data strongly suggest that there are key social interaction defects that are irreversible by restoration of nNOS.

The repetitive and stereotyped behaviors are widely known as core and defining features of ASD [24]. Many lines of evidence have shown that VPA-treated mice exhibited the increase in self-grooming and marble-burying [23, 24]. In support of this findings, we show that LV-nNOS overexpression and L-arginine treatment-activating PI3K-AKT-mTOR signaling restored the normal levels of marble-burying in experimental animals. In addition, individuals with ASD are at a risk for developing anxiety [29]. A growing body of studies has supported the notion that nNOS has a dominant role in anxiety role [41, 42]. Data with L-arginine would suggest the use of treating anxiety [42]. In agreement with previous findings, we confirm re-expression of nNOS reverses their repetitive/stereotyped behaviors and anxiety-like traits, indicating that restoring nNOS can correct all behavioral phenotypes.

Our experiments revealed that surface protein of AMPA receptor subunits GluA4 increased in mice exposed to

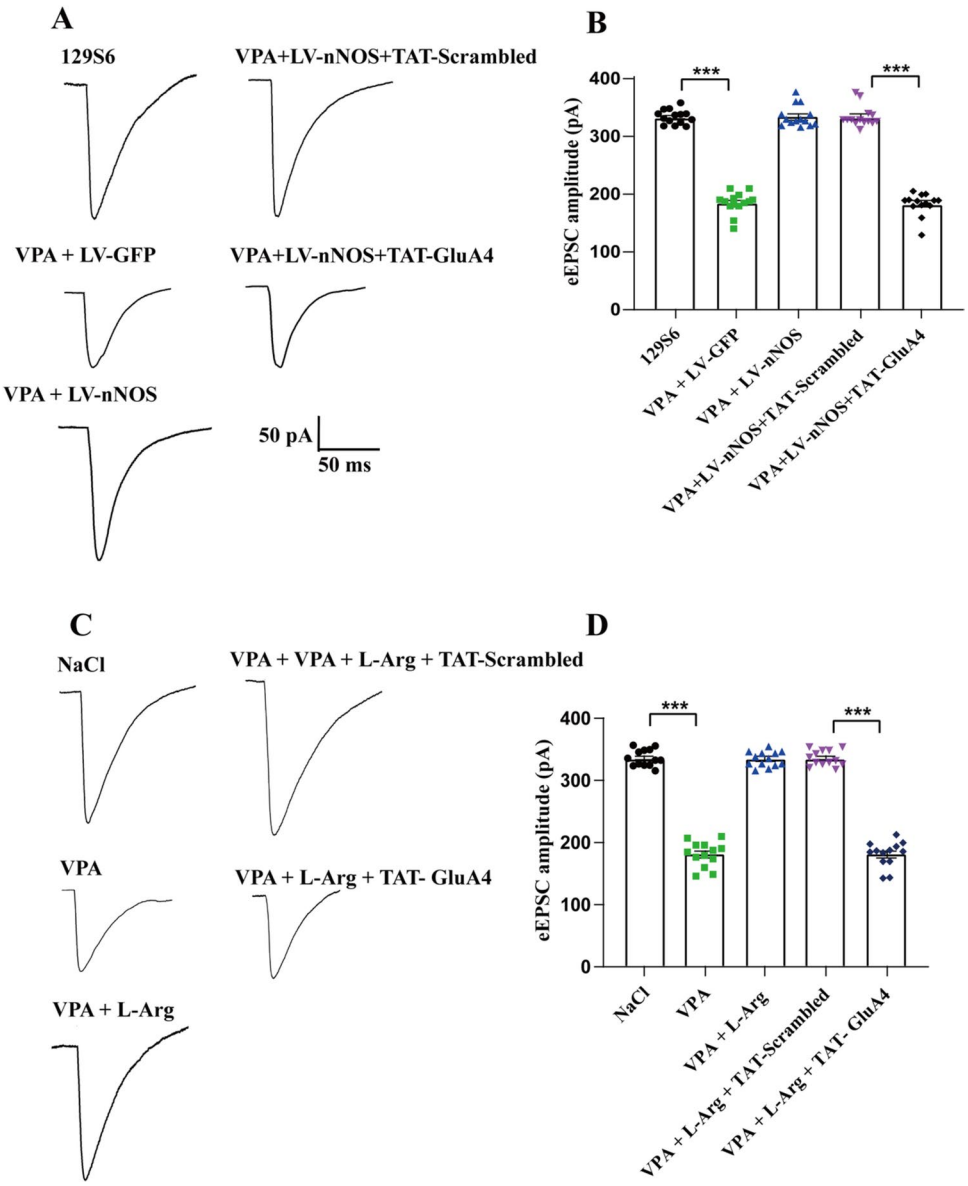

Fig. 5 Restoration of nNOS expression increases evoked AMPA-mediated excitatory synaptic currents (AMPA eEPSCs) of nNOS-expressing interneurons in VPA-treated mice. Representative traces of AMPA eEPSC (**A**) and summary graphs showing the amplitude (**B**) of eEPSCs for129S, VPA + LV-GFP, VPA + LV-nNOS, VPA + LV-nNOS + TAT-scrambled, and VPA + LV-nNOS + TAT-GluA4 group. Representative traces of AMPA eEPSC (**C**) and summary graphs showing the amplitude (**D**) of AMPA eEPSCs for NaCl, VPA, VPA + L-Arg, VPA + L-Arg + TAT-scrambled, and VPA + L-Arg + TAT-GluA4 group. $n = 14$ slices from 6 mice in each group. $^{***}p < 0.001$ one-way ANOVA. Data are presented as means ± SEM

LV-nNOS and L-arginine activating PI3K-Akt-mTOR signaling, indicating that re-expression of nNOS rescues ASD-like behaviors through GluA4 subunits during postsynaptic activation. Further, many proteins interact with AMPA receptor subunits and affect their synaptic localization. GluA4 receptors are continuously transported in and out of synapses by membrane trafficking, which involves insertion and internalization via specific vesicles [12]. Narp is a neuronal immediate early gene belonging to a member of the neuronal pentraxin family. It was demonstrated that Narp stabilizes postsynaptic GluA4 in the parvalbumin-containing interneurons [12, 43]. We have previous shown that surface proteins of Narp and GluA4 in nNOS interneurons were decreased in mice treated with VPA [10]. Currently, we found that cell surface Narp and GluA4 expression was increased in nNOS re-expression-treated mice, whereas total protein levels did not change, indicating increased GluA4 trafficking from intracellular pools to the cell surface. Similar to our findings, it was reported that Narp decrease could be related to the massive GluA4 decrease in the prefrontal cortex of fluoxetine-treated mice [44]. TAT-GluA4 interfering peptides were remarkably effective at preventing reduction of the surface expression of Narp and GluA4 in re-expression in nNOS-treated mice caused by VPA. Therefore, nNOS re-expression may increase the trafficking of GluA4 subunits, resulting in improving symptoms of ASD-like behaviors.

Previous studies have indicated dysfunctional excitatory synaptic transmission in interneurons in mouse model of ASD [12, 45, 46]. In particular, knockdown of contactin-associated protein-like 2 (CNTNAP2) or belson helper integration site-1 (AHI1) in layer 2/3 pyramidal neurons of the

developing mouse prefrontal cortex reduced excitatory synaptic transmission, e.g., decreased amplitude of evoked EPSCs, and impaired social interaction [7]. Guo et al. reported that Shank3 deletion induced AMPA receptor-mediated synaptic impairments in the anterior cingulate gyrus [6]. Likewise, Vyas et al. demonstrated that Shank3-deficient human neurons have reduced AMPA-mediated synaptic transmission [5]. Further, in the present work, we determined the effect of restoring nNOS on synaptic transmission in the BLA and found that nNOS re-expression increased amplitude of AMPA receptor-mediated mEPSC and eEPSC of nNOS-containing interneurons in the VPA-treated mice. These findings are consistent with previous reports that AMPA receptors are targets for treating ASD-associated phenotypes. Kim et al. reported that AMPA receptor modulators (antagonist for VPA mice) can improve autistic symptoms by normalizing the aberrant excitatory transmission in the respective animal models [47]. Pharmacological enhancement of postsynaptic AMPA receptor function effectively restored impaired social behavior in both CNTNAP2- and AHI1-knockdown mice [7]. TAT-GluA4 interfering peptides were remarkably effective at preventing AMPA-mediated mEPSC and eEPSC amplitude in nNOS interneurons in re-expression nNOS-treated animal caused by VPA.

Further, GluA4 is dramatically reduced in *Narp-/-* mice with consequent reductions in the PV-expressing interneuron AMPA receptor function (Chang et al., 2010). Very recently, an elegant study revealed that knockdown of Narp decreased AMPA receptor EPSCs in dorsal CA1 neurons after retrieval [13]. It was shown that Narp stabilizes postsynaptic GluA4 in interneurons to enhance excitatory synaptic transmission [12, 43]. Following this line of reasoning, we conclude that restoration of nNOS enhances GluA4 AMPA receptor-mediated excitatory synaptic transmission, thereby inducing alleviation of behavioral deficits of ASD.

To summarize, we demonstrate that the virus-mediated overexpression of nNOS and L-arginine administration activating PI3K-AKT-mTOR signaling contributes to attenuation of the core ASD-associated deficits ranging from the enhanced excitatory synaptic transmission to behavioral features that are associated with multiple symptomatic domains. The increased Narp-mediated GluA4 AMPA receptors trafficking to the plasma membrane by nNOS re-expression can be used as an optimal target for autistic behaviors. Our study provides evidence that may aid in the development of alternative approaches to treat ASD through GluA4-containing AMPA receptor-mediating excitatory neurotransmission. Future studies could aim to dissect the circuit-related mechanisms by which the BLA regulates ASD-like phenotypes by restoring nNOS expression. It would not only provide valuable insights into the neural substrates underlying behavioral aberration characteristics to ASD but also help develop novel targeted therapeutics for ASD by tuning the BLA-mediated circuit.

Author Contribution XW designed the research and wrote the manuscript. KZ conducted the viral infusion surgeries. SL and SH performed the behavioral characterization and analyzed the data. YD, DM, and CG carried out western blotting. XW performed electrophysiological experiments and analyzed the data as well. XW and YZ supervised all aspects of the research. All authors have read and approved the final version of the manuscript.

Funding We gratefully acknowledge the sponsorship from the National Natural Science Foundation of China (81901387), the Scientific and Technological Project of Henan (232102311006, 212102310034, 232102310077), the Medical Science and Technique Program of Henan (LHGJ20210632), the Natural Science Foundation of Henan (232300421086), the Henan Neural Development Engineering Research Center for Children Foundation (SG202202), and the Joint Fund of Henan Provincial Science and Technology Research (225200810114).

Data Availability All data generated for this study are available on request to the corresponding author.

Declarations

Ethics Approval and Consent to Participate The animal study was reviewed and approved by the Institutional Animal Ethics Committee of Zhengzhou University, following the NIH Guidelines for the Care and Use of Laboratory Animals.

Consent for Publication Not applicable.

Competing Interests The authors declare no competing interests.

References

1. Wang X, Gao C, Zhang Y, Hu S, Qiao Y, Zhao Z et al (2021) Overexpression of mGluR7 in the prefrontal cortex attenuates autistic behaviors in mice. Front Cell Neurosci 15:689611
2. Gao Y, Sun J, Cheng L, Yang Q, Li J, Hao Z et al (2022) Altered resting state dynamic functional connectivity of amygdala subregions in patients with autism spectrum disorder: a multi-site fMRI study. J Affect Disord 312:69–77
3. Kim S, Kim YE, Song I, Ujihara Y, Kim N, Jiang YH et al (2022) Neural circuit pathology driven by Shank3 mutation disrupts social behaviors. Cell Rep 39(10):110906
4. Chiola S, Napan KL, Wang Y, Lazarenko RM, Armstrong CJ, Cui J et al (2021) Defective AMPA-mediated synaptic transmission and morphology in human neurons with hemizygous SHANK3 deletion engrafted in mouse prefrontal cortex. Mol Psychiatry 26(9):4670–4686
5. Vyas Y, Lee K, Jung Y, Montgomery JM (2020) Influence of maternal zinc supplementation on the development of autism-associated behavioural and synaptic deficits in offspring Shank3-knockout mice. Mol Brain 13(1):110
6. Guo B, Chen J, Chen Q, Ren K, Feng D, Mao H et al (2019) Anterior cingulate cortex dysfunction underlies social deficits in Shank3 mutant mice. Nat Neurosci 22(8):1223–1234

7. Sacai H, Sakoori K, Konno K, Nagahama K, Suzuki H, Watanabe T et al (2020) Autism spectrum disorder-like behavior caused by reduced excitatory synaptic transmission in pyramidal neurons of mouse prefrontal cortex. Nat Commun 11(1):5140
8. Niescier RF, Lin YC (2021) The potential role of AMPA receptor trafficking in autism and other neurodevelopmental conditions. Neuroscience 479:180–191
9. Ganea DA, Dines M, Basu S, Lamprecht R (2015) The membrane proximal region of AMPA receptors in lateral amygdala is essential for fear memory formation. Neuropsychopharmacology 40(12):2727–2735
10. Wang X, Yang Z, Fang S, Zhang Y, Guo J, Gou L (2021) Declining levels of specialized synaptic surface proteins in nNOS-expressing interneurons in mice treated prenatally with valproic acid. Neurochem Res 46(7):1794–1800
11. Wu QL, Gao Y, Li JT, Ma WY, Chen NH (2022) The role of AMPARs composition and trafficking in synaptic plasticity and diseases. Cell Mol Neurobiol 42(8):2489–2504
12. Pelkey KA, Barksdale E, Craig MT, Yuan X, Sukumaran M, Vargish GA et al (2015) Pentraxins coordinate excitatory synapse maturation and circuit integration of parvalbumin interneurons. Neuron 85(6):1257–1272
13. Wang Z, Jin T, Le Q, Liu C, Wang X, Wang F et al (2019) Retrieval-driven hippocampal NPTX2 plasticity facilitates the extinction of cocaine-associated context memory. Biol Psychiatry 87(11):979–991
14. Wang X, Liu C, Wang X, Gao F, Zhan RZ (2017) Density and neurochemical profiles of neuronal nitric oxide synthase-expressing interneuron in the mouse basolateral amygdala. Brain Res 1663:106–113
15. Wei J-A, Han Q, Luo Z, Liu L, Cui J, Tan J et al (2022) Amygdala neural ensemble mediates mouse social investigation behaviors. Natl Sci Rev
16. Armstrong C, Magnuson EK, Soltesz I (2012) Neurogliaform and Ivy cells: a major family of nNOS expressing GABAergic neurons. Front Neural Circ 6:23
17. Li G, Stewart R, Canepari M, Capogna M (2014) Firing of hippocampal neurogliaform cells induces suppression of synaptic inhibition. J Neurosci 34(4):1280–1292
18. Wang X, Zhang Y, Cheng W, Gao Y, Li S (2021) Decreased excitatory drive onto hilar neuronal nitric oxide synthase expressing interneurons in chronic models of epilepsy. Brain Res 1764:147467
19. Wang X, Guo J, Song Y, Wang Q, Hu S, Gou L et al (2018) Decreased number and expression of nNOS-positive interneurons in basolateral amygdala in two mouse models of autism. Front Cell Neurosci 12:251–257
20. Dai L, Weiss RB, Dunn DM, Ramirez A, Paul S, Korenberg JR (2021) Core transcriptional networks in Williams syndrome: IGF1-PI3K-AKT-mTOR, MAPK and actin signaling at the synapse echo autism. Hum Mol Genet 30(6):411–429
21. Rivell A, Mattson MP (2019) Intergenerational metabolic syndrome and neuronal network hyperexcitability in autism. Trends Neurosci 42(10):709–726
22. Bertoni A, Schaller F, Tyzio R, Gaillard S, Santini F, Xolin M et al (2021) Oxytocin administration in neonates shapes hippocampal circuitry and restores social behavior in a mouse model of autism. Mol Psychiatry 26(12):7582–7595
23. Klibaite U, Kislin M, Verpeut JL, Bergeler S, Sun X, Shaevitz JW et al (2022) Deep phenotyping reveals movement phenotypes in mouse neurodevelopmental models. Mol Autism 13(1):12
24. Moutin E, Sakkaki S, Compan V, Bouquier N, Giona F, Areias J et al (2021) Restoring glutamate receptosome dynamics at synapses rescues autism-like deficits in Shank3-deficient mice. Mol Psychiatry 26(12):7596–7609
25. Wang X, Guo Z, Mei D, Zhang Y, Zhao S, Hu S et al (2022) The GluN2B-Trp373 NMDA receptor variant is associated with autism-, epilepsy-related phenotypes and reduces NMDA receptor currents in rats. Neurochem Res 47(6):1588–1597
26. Wang X, Mei D, Gou L, Zhao S, Gao C, Guo J et al (2023) Functional evaluation of a novel GRIN2B missense variant associated with epilepsy and intellectual disability. Neuroscience 526:107–120
27. Hu J, Ng YK, Chin CM, Ling EA (2008) Effects of l-arginine and N(G)-nitro-l-arginine methyl ester treatments on expression of neuronal nitric oxide synthase in the guinea-pig bladder after partial bladder outlet obstruction. Neuroscience 151(3):680–691
28. Dingemans AJM, Truijen KMG, Ven Svd, Bernier R, Bongers EMHF, Bouman A et al (2022) The phenotypic spectrum and genotype-phenotype correlations in 106 patients with variants in major autism gene CHD8. Transl Psychiatry 12(1):421
29. Yarger HA (2022) Anxiety-amygdala associations: novel insights from the first longitudinal study of autistic youth with distinct anxiety. Biol Psychiat 91(11):e41–e43
30. Zheng Z, Keifer J (2014) Sequential delivery of synaptic GluA1- and GluA4-containing AMPA receptors (AMPARs) by SAP97 anchored protein complexes in classical conditioning. J Biol Chem 289(15):10540–10550
31. Zhu JW, Zou MM, Li YF, Chen WJ, Liu JC, Chen H et al (2020) Absence of TRIM32 leads to reduced GABAergic interneuron generation and autism-like behaviors in mice via suppressing mTOR signaling. Cereb Cortex (New York, NY : 1991) 30(5):3240–3258
32. Gazestani VH, Pramparo T, Nalabolu S, Kellman BP, Murray S, Lopez L et al (2019) A perturbed gene network containing PI3K–AKT, RAS–ERK and WNT–β-catenin pathways in leukocytes is linked to ASD genetics and symptom severity. Nat Neurosci 22(10):1624–1634
33. Russo AJ (2015) Decreased phosphorylated protein kinase B (Akt) in individuals with autism associated with high epidermal growth factor receptor (EGFR) and low gamma-aminobutyric acid (GABA). Biomark Insights 10:89–94
34. Nicolini C, Ahn Y, Michalski B, Rho JM, Fahnestock M (2015) Decreased mTOR signaling pathway in human idiopathic autism and in rats exposed to valproic acid. Acta Neuropathol Commun 3:3
35. Xing X, Wu K, Dong Y, Zhou Y, Zhang J, Jiang F et al (2020) Hyperactive Akt-mTOR pathway as a therapeutic target for pain hypersensitivity in Cntnap2-deficient mice. Neuropharmacology 165:107816
36. Shih PY, Fang YL, Shankar S, Lee SP, Hu HT, Chen H et al (2022) Phase separation and zinc-induced transition modulate synaptic distribution and association of autism-linked CTTNBP2 and SHANK3. Nat Commun 13(1):2664
37. Mishra A, Singla R, Kumar R, Sharma A, Joshi R, Sarma P et al (2022) Granulocyte colony-stimulating factor improved core symptoms of autism spectrum disorder via modulating glutamatergic receptors in the prefrontal cortex and hippocampus of rat brains. ACS Chem Neurosci 13:2942–2961
38. Barreto LE, Morales M (2016) The PI3K signaling pathway as a pharmacological target in autism related disorders and schizophrenia. Mol Cell Ther 4:2

39. Cupolillo D, Hoxha E, Faralli A (2016) Autistic-like traits and cerebellar dysfunction in Purkinje cell PTEN knock-out mice. Neuropsychopharmacology. 41(6):1457–1466
40. Mellios N, Feldman DA, Sheridan SD, Ip JPK, Kwok S, Amoah SK et al (2018) MeCP2-regulated miRNAs control early human neurogenesis through differential effects on ERK and AKT signaling. Molecular psychiatry. 23(4):1051–1065
41. Zhu LJ, Xu C, Ren J, Chang L, Zhu XH, Sun N et al (2020) Dentate nNOS accounts for stress-induced 5-HT1A receptor deficiency: implication in anxiety behaviors. CNS Neurosci Ther 26(4):453–464
42. Zhou QG, Zhu XH, Nemes AD, Zhu DY (2018) Neuronal nitric oxide synthase and affective disorders. IBRO Rep 5:116–132
43. Chang MC, Park JM, Pelkey KA, Grabenstatter HL, Xu D, Linden DJ et al (2010) Narp regulates homeostatic scaling of excitatory synapses on parvalbumin-expressing interneurons. Nat Neurosci 13(9):1090–1097
44. Heinrich IA, Freitas AE, Wolin IAV, Nascimento APM, Walz R, Rodrigues ALS et al (2021) neuronal activity regulated pentraxin (narp) and GluA4 subunit of AMPA receptor may be targets for fluoxetine modulation. Metab Brain Dis 36(4):711–722
45. Mei Y, Monteiro P, Zhou Y, Kim JA, Gao X, Fu Z et al (2016) Adult restoration of Shank3 expression rescues selective autistic-like phenotypes. Nature 530(7591):481–484
46. Cao W, Lin S, Xia QQ, Du YL, Yang Q, Zhang MY et al (2018) Gamma oscillation dysfunction in mPFC leads to social deficits in neuroligin 3 R451C knockin mice. Neuron 97(6):1253–1260
47. Kim JW, Park K, Kang RJ, Gonzales ELT, Kim DG, Oh HA et al (2019) Pharmacological modulation of AMPA receptor rescues social impairments in animal models of autism. Neuropsychopharmacology 44(2):314–332